Solar MHD Theory and Observations: A High Spatial Resolution Perspective
ASP Conference Series, Vol. 354, 2006
Uitenbroek, Leibacher, and Stein

Active Region Magnetic Fields in the Solar Interior

W. P. Abbett and G. H. Fisher
Space Sciences Laboratory, University of California, Berkeley, CA 94720-7450

Abstract. We present a brief review of recent efforts to understand the life-cycle of active region magnetic fields with an emphasis on what photospheric observations can tell us about the evolution of large-scale magnetic structures deep in the convective interior. A critical component of these efforts is to understand the dynamic connection between magnetic fields (at both large and small scales) observed threading the solar atmosphere and their sub-surface counterparts. We conclude our survey by presenting early results from a new numerical model capable of self-consistently incorporating both sub-photospheric layers and the low solar corona into a single computational domain.

1. Why Study Active Regions?

Many, if not all, of the most spectacular manifestations of solar activity — for example, coronal mass ejections (CMEs) and solar flares — are associated with active regions. It is well known that CMEs and flares accelerate particles to high energies, and that these solar energetic particles (SEPs) can propagate along magnetic field lines toward the Earth's magnetosphere where they can adversely affect a variety of ground and spaced based systems, including (but not limited to) the operations of satellites and commercial aircraft (Knowles et al. 2001; Getley 2004), power grids and cellular telephone service (Forbes & St. Cyr 2004). Thus, there is a keen interest in being able to accurately model and predict "space weather" — to develop the scientific understanding and numerical capability to simulate the Sun-Earth system in the same way that meteorologists use numerical models to understand and predict terrestrial weather (Wright et al. 1995). Unfortunately, the least understood component of the Sun-Earth system is the solar atmosphere — precisely where geo-effective eruptive events are thought to originate. It is this region that necessarily forms the critical driving boundary for physics-based models of the Sun-Earth system (Abbett et al. 2004). Without accurate observations and a physical understanding of the active solar atmosphere, and the means to incorporate this knowledge into numerical models of solar atmosphere and heliosphere, we cannot expect to improve our ability to understand and predict space weather beyond simplified analytic, empirical, or stochastic treatments.

It is widely accepted that CMEs are magnetically driven phenomena that originate in the low corona (Forbes & Isenberg 1991; Antiochos et al. 1999). Yet, the important changes in coronal magnetic topology that can lead to eruptive events are governed, at least in part, by magnetic fields and flows at and below the visible surface (Fan & Gibson 2004; Lynch et al. 2004; Linker et al. 2005).

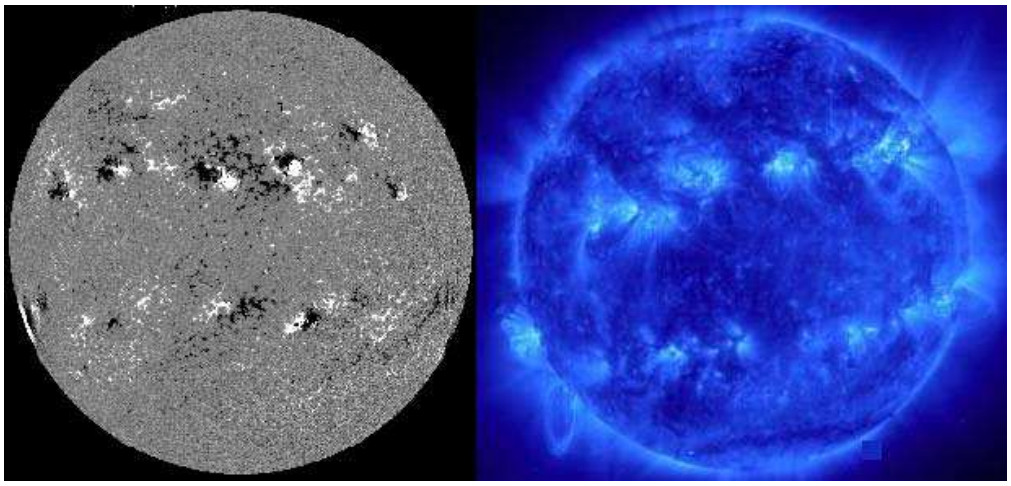

Figure 1. Left: Full disk line-of-sight magnetogram taken in May of 2000 by the Michelson Doppler Imager (MDI) on the Solar and Heliospheric Observatory (SOHO). Dark regions represent magnetic polarities directed away from the observer, and light regions represent polarities directed toward the observer (grey is nominally zero). Right: An image of coronal plasma at ∼1.3 MK taken during a time of heightened solar activity by the Extreme Ultraviolet Imaging Telescope (EIT) on SOHO. Images courtesy of the SOHO-EIT and SOHO-MDI consortia.

Thus, we must ask: How well do we understand these sub-surface structures? What can we infer from theoretical and computational models of the sub-surface evolution of active region magnetic fields? How well do these models compare with observations? In this brief review, we provide a general summary of the current understanding of specific topics directly relevant to each of these questions. We begin by describing the observed, global properties of active regions at the solar surface, then work our way toward the many models that attempt to explain these observations.

2. Properties of Active Regions

Any model of active region magnetic fields (and the solar dynamo) must be entirely consistent with the observed characteristics of active regions at both local and global scales. What are some of these essential observational characteristics? Many were discovered early in the 20th century, and have withstood the test of time (see *e.g.*, Hale et al. 1919): (1) Most active regions exhibit a relatively simple bipolar structure, and are oriented (on average) in the azimuthal direction (Hale's Law). (2) Active regions tend to be confined in symmetric latitudinal bands across the solar equator. These bands emerge $\sim 10^{\circ}$ above or below the equator and move poleward as the 11-year solar cycle progresses. (3) The leading polarities of a given hemisphere (those in the direction of solar rotation) are the same, and oppose those of the opposite hemisphere (the polarity order reverses at the beginning of each new solar cycle). (4) On average, leading polarities of active regions are positioned closer to the equator than their trail-

ing counterparts (though convective turbulence imparts a large variation about the average). In addition, the mean "tilt angle" – the angle defined by a line drawn between the magnetic center of each polarity and a line parallel to the solar equator – increases with latitude (Joy's Law). (5) The magnetic structures comprising the trailing polarities of newly-formed active regions tend to be less organized and more readily susceptible to the effects of turbulent convection than the more concentrated leading polarities. Many of these characteristics are evident in Figure 1, which shows the photospheric line-of-sight (LOS) magnetic field and coronal X-ray emission over the entire solar disk during two particularly active times.

The azimuthal orientation of active regions as described by Hale's Law argues for the presence of a strong, large-scale sub-surface toroidal magnetic field. In addition, the persistence of Hale's Law implies that this field must be maintained over periods of time comparable to the solar cycle. A natural place for these fields to be stored is at or near the place where they are thought to be generated – the tachocline (see *e.g.* Kosovichev 1996; Corbard et al. 1999), where the differentially rotating convection zone transitions into the stable radiative layers, and the large-scale solar dynamo is thought to operate (Parker 1979; van Ballegooijen 1982; Dikpati & Charbonneau 1999). Here, strong magnetic fields can be stored against the effects of magnetic buoyancy, but are still subject to hydrodynamic, radiative or magnetic perturbations that may cause a portion of the toroidal field to ascend toward the surface (see *e.g.*, Cattaneo & Hughes 1988; Fan & Fisher 1996; Wissink et al. 2000; Fan 2001). It is also argued that convection alone can pin down the large-scale azimuthally directed fields through a process called "turbulent pumping" (Dorch & Nordlund 2001). Either way, if a toroidal field resides near the base of the convection zone, it must be able to make its way cohesively through the entirety of the turbulent interior if it is to emerge in a manner consistent with observations of active region magnetic fields at the photosphere.

Great progress has been made in recent years understanding the conditions under which isolated magnetic structures capable of being progenitors of a strong active regions can survive their ascent through the turbulent, stratified layers of the solar convection zone. If these structures are unable to retain the cohesion necessary to appear as bipoles at the solar surface, the standard picture described above must be called into question. We begin a summary of these efforts by describing one of the first theoretical models of active region-scale sub-surface magnetic fields that put forth a physically consistent explanation of a number of the observational characteristics of active regions described above: the Thin Flux Tube (TFT) model (see Spruit 1981).

3. The Thin Flux Tube Model

In the TFT approach, sub-surface active region-scale magnetic fields are viewed as magnetic flux tubes propagating through a field-free model convection zone. The TFT approximation is based on the following assumptions: First, as the flux tube moves, it retains its identity – the tube remains cohesive and does not disperse or fragment. Second, the tube is "thin"; that is, its cross-section is small relative to all other relevant length scales of the problem. Third, quasi-static

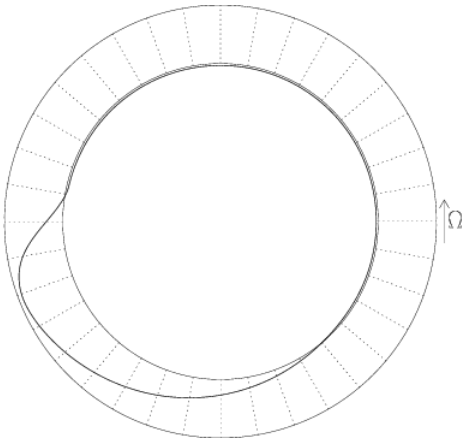

Figure 2. An example of a thin flux tube calculation from Caligari et al. (1995). Shown is a projection of the thin flux tube onto the equatorial plane. Note how the leading leg is less vertically inclined than the trailing leg – it is is easy to see how the leading polarity of an active region could move away from the neutral line more rapidly than the trailing leg during the emergence process.

pressure balance is maintained across the diameter of the tube at all times. If we further assume that the thin flux tube is untwisted (the magnetic field $\mathbf{B}$ is directed along the axis of the tube) we can derive a TFT equation of motion:

$$\rho_i \frac{D\mathbf{v}}{Dt} = \mathbf{F}_B + \mathbf{F}_T + \mathbf{F}_C + \mathbf{F}_D. \tag{1}$$

Here, $\mathbf{F}_B = g(\rho_e - \rho_i)\mathbf{r}$ refers to the magnetic buoyancy force, $\mathbf{F}_T = B^2/(8\pi)\boldsymbol{\kappa}$ the force due to magnetic tension, $\mathbf{F}_C = -2\rho_i\,\boldsymbol{\Omega} \times \mathbf{v}$ the Coriolis force (the vector $\boldsymbol{\Omega}$ denotes the angular velocity about the Sun's axis of rotation), and $\mathbf{F}_D = -\rho_e(C_D/\sqrt{\pi\Phi/B})|\mathbf{v}_\perp|\mathbf{v}_\perp$ the force resulting from aerodynamic drag. The quantity Φ refers to the magnetic flux threading the cross-section of the tube. The gas density external to the tube and in the tube's interior are denoted ρ_e and ρ_i respectively, and $\mathbf{r}$ and $\boldsymbol{\kappa}$ are the unit vector in the radial direction (opposing the gravitational acceleration $\mathbf{g}$) and the curvature vector respectively (the curvature vector is explicitly defined as $\boldsymbol{\kappa} = d^2\mathbf{R}/ds^2$, where $\mathbf{R}$ denotes the position of the axis of the flux tube, and ds denotes an infinitesimal path length along $\mathbf{R}$). In the expression that characterizes aerodynamic drag, $\mathbf{v}_\perp$ refers to the normal component of the velocity difference between the tube itself, and plasma entrained within the tube. C_D is a drag coefficient (typically set to unity).

The TFT treatment has provided insight into many of the physical processes underlying active region evolution. The evolution of thin flux tubes embedded in spherical rotating model convection zones have led to the following conclusions: (1) Based on observations of the latitude of emergence of active regions at the visible surface, the magnetic field strength of a toroidal layer at the base of the convection zone must be between 3×10^4 and 10^5 G (Choudhuri 1989; D'Silva & Howard 1993; D'Silva & Choudhuri 1993; Fan et al. 1993; Caligari et al. 1995; Fan

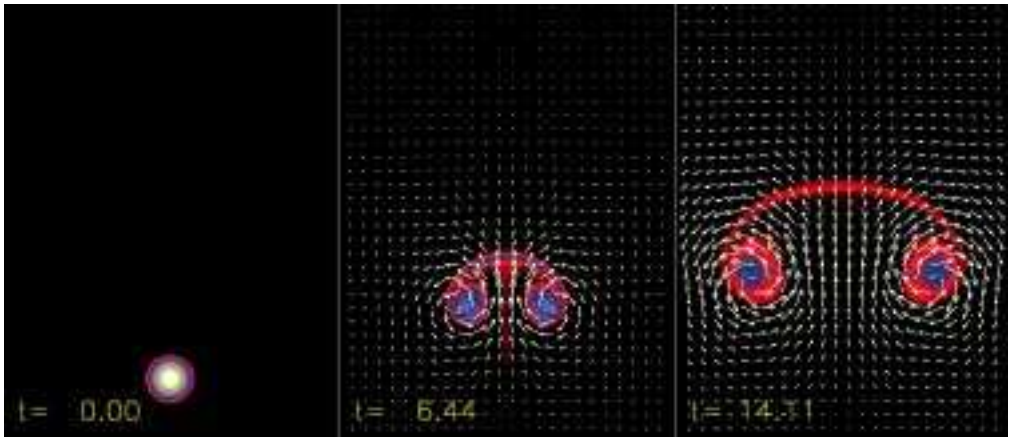

Figure 3. An MHD simulation from Fan et al. (1998) showing the fragmentation of an axially symmetric, untwisted flux tube.

& Fisher 1996). Note that these values are higher than the equipartition value relative to the expected kinetic energy density due to convective motions. In addition, the "zone of avoidance" (the tendency for active regions not to emerge at the solar equator) can be explained in terms of the Coriolis force acting on flux tubes during their ascent. (2) Joy's law can also be explained in terms of the Coriolis force acting on rising, expanding flux ropes (D'Silva & Howard 1993; D'Silva & Choudhuri 1993; Fisher, Fan, & Howard 1995). Assuming this is the physical mechanism behind the dependence of active region tilts on latitude, one can derive an expression for the tilt angle α of the form, $\alpha = \Phi^{1/4} \sin\theta$. Here, the dependence on latitude θ is Joy's law, but the dependence on magnetic flux Φ was a prediction of the TFT model, and was successfully tested against observations (Fisher, Fan, & Howard 1995; Tian et al. 2003). (3) The TFT model provides a physical explanation for asymmetric spot motions and morphological asymmetries (van Driel-Gesztelyi & Petrovay 1990; Moreno-Insertis, Schüssler, & Caligari 1994; Caligari et al. 1995; Fan & Fisher 1996). For example, the more rapid motion of the leading polarity away from the neutral line can be understood in terms of the tendency of plasma entrained within the flux tube to conserve its angular momentum – this gives rise to a distorted Ω-shaped loop whose leading leg is less vertically inclined than its trailing leg (see Figure 2). The TFT approximation has also been used to understand the dispersion of tilt versus AR size (Longcope & Fisher 1996), and the helicity distributions of active regions with latitude (Longcope et al. 1998).

4. MHD Simulations of Active Regions Below the Surface

Of course, it is desirable to treat the physics of active region-scale magnetic fields in a more realistic fashion. The next logical step is to move beyond the TFT approximation and numerically solve the magnetohydrodynamic (MHD) system of equations in a domain that encompasses the deep layers of the convection zone. The first calculations of this type assumed axial symmetry (re-

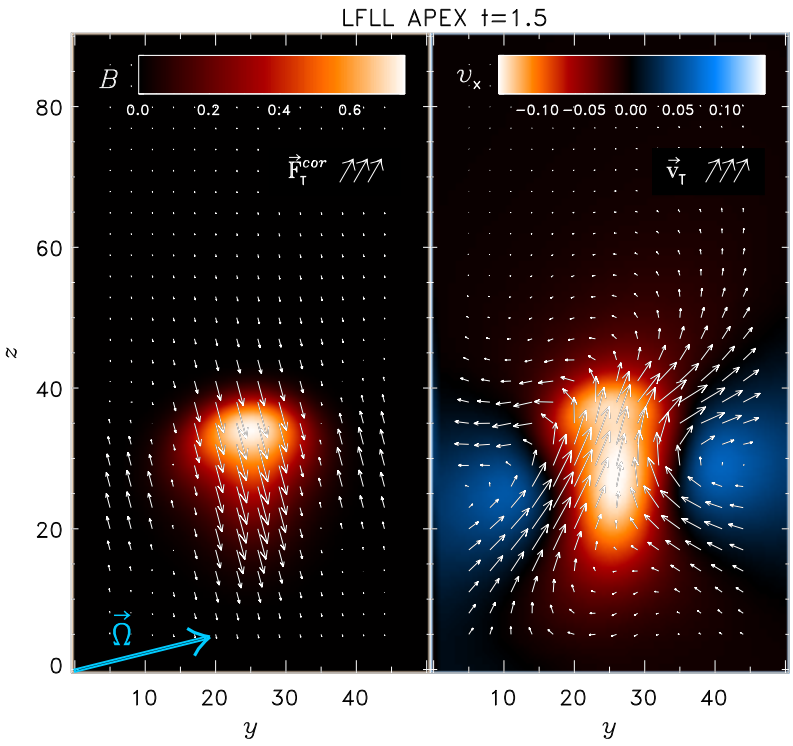

Figure 4. An MHD simulation from Abbett et al. (2001) showing the magnetic field and flows along a cross-sectional slice at the apex of an Ω-loop. Coriolis forces affect the flow pattern along the tube, and as a result, fragmentation is suppressed.

quiring only a two-dimensional MHD calculation), and considered the buoyant rise of untwisted flux ropes in the Boussinesq (acoustically filtered, no stratification), anelastic (acoustically filtered, with stratification), and fully-compressible regimes (see *e.g.*, Moreno-Insertis & Emonet 1996; Longcope et al. 1996; Emonet & Moreno-Insertis 1998; Fan et al. 1998). These studies found that without a substantial azimuthal component of the field – far more field line twist than is, on average, observed at the solar surface (Pevtsov, Canfield, & Metcalf 1995) – flux tubes fragment long before they can reach the photosphere. This is evident in Figure 3, where an untwisted flux tube is seen to fragment into two separate flux concentrations centered along oppositely directed vortices. It is the hydrodynamic interaction between these vortices that forces their separation, and prevents the emergence of any significant amount of magnetic flux through the surface.

As computational resources improved, it was possible to relax the assumption of axial symmetry, and to repeat these calculations in a three-dimensional geometry. The results of MHD simulations in the anelastic approximation (see Lantz & Fan (1999) and references therein for a detailed derivation of the anelastic system of equations) of magnetic flux tubes in a three-dimensional, stratified model convection zone are substantially different than the two-dimensional calculations (see Abbett et al. 2000): much less field line twist is required for a flux tube to remain cohesive during its ascent, since the vortex interaction is limited to a finite region near the apex of an Ω-shaped loop. In addition, differential circulation between the apex and foot points of an Ω-loop leads to an introduction of new magnetic twist in each leg of a loop fragment that further reduces the circulation near the apex, further suppressing the tendency for the loop to fragment. If the effects of solar rotation are included in the models (see Abbett et al. 2001), it can be shown that the Coriolis force also acts to suppress the degree of apex fragmentation of an Ω-loop. These calculations show that a flux tube can retain its cohesion during its buoyant rise through the convection zone even in the absence of field-line twist (see Figure 4), thus resolving the apparent contradiction between the results of the two-dimensional models and observations. Three-dimensional MHD simulations have also confirmed some of the predictions of the TFT models; namely, that the leading polarity of an emerging active region is positioned closer to the equator than the trailing polarity, and that the trailing leg of the loop is oriented more vertically than the leading leg (see Figure 5).

Yet in each of the previous studies, the model convection zone, while highly stratified, is not turbulent. One of the first attempts to simulate the effects of convective motion on active region scale flux ropes in three spatial dimensions was that of Dorch et al. (2001) who used a fully compressible MHD code to investigate the amount of magnetic flux that could be advected away from the core of an active region-scale flux rope. A larger parameter space study was performed by Fan et al. (2003) in the anelastic regime. The primary conclusion of this study was that the axial field strength of a flux rope B must be greater than a critical value $B_c = B_{eq}\sqrt{H_P/a}$ (where H_P, a, and B_{eq} refer to the local pressure scale height, the tube's radius, and the equipartition magnetic field strength relative to the kinetic energy density of strong convective flows) in order for the magnetic buoyancy of the flux rope to overcome the hydrodynamic forces due to convection. For the limiting case where the field is weak ($B \ll B_c$),

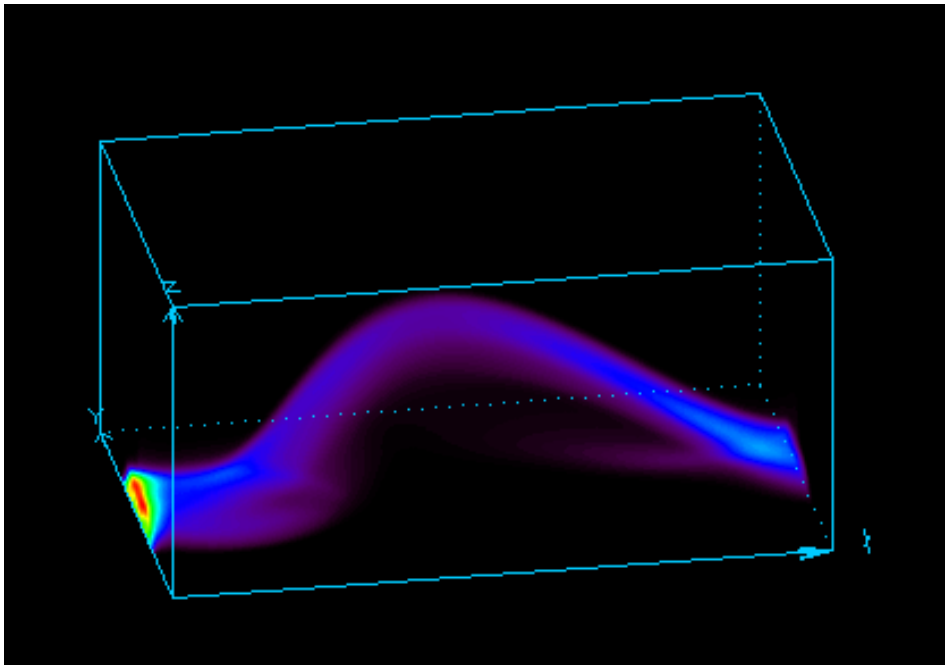

Figure 5. An MHD simulation from Abbett et al. (2001) showing the effects of the Coriolis force on the geometry of a buoyant Ω-loop.

convective flows dominate the evolution of sub-surface magnetic structures, and Ω-loops of any shape quickly lose cohesion (see Figure 6). However, for cases where the field is strong relative to B_c, the loop itself disrupts the characteristic convective flow pattern, evolving as if the convective turbulence were absent (consistent with studies where the model convection zone is non-turbulent).

One can then ask the question: for relatively weak active region magnetic fields ($0.1B_{eq} < B < 2B_{eq}$) where the axial field strength of an Ω-loop is slightly less than the critical value $B_c \sim 3B_{eq}$, on average, how much magnetic flux is transported to the base of the convection zone as a result of interactions with the asymmetric vertical flowfield characteristic of stratified convection? This question is highly relevant to *e.g.*, mean field dynamo models (Parker 1993; Charbonneau & MacGregor 1997). In this weak field regime, high resolution, fully compressible MHD simulations of penetrative convection have shown that magnetic flux is preferentially transported downward (against the effects of magnetic buoyancy) by convective flows into the stably stratified overshoot region (Tobias et al. 1998, 2001; Dorch & Nordlund 2001). In the absence of an overshoot layer, this downward "turbulent pumping" of magnetic flux is somewhat less dramatic. In fact, over the short lifetime of a typical flux tube (several convective turnover times before the tube loses its identity and is shredded by convective flows) Abbett et al. (2004) find that there is no systematic net transport of magnetic flux downward toward the base of the computational domain — if anything, there is a slight initial tendency for flux to be transported upward toward the surface. Over much longer time scales, however, the simulations of Abbett et al. (2004) do indeed show a net downward pumping of flux, but in the

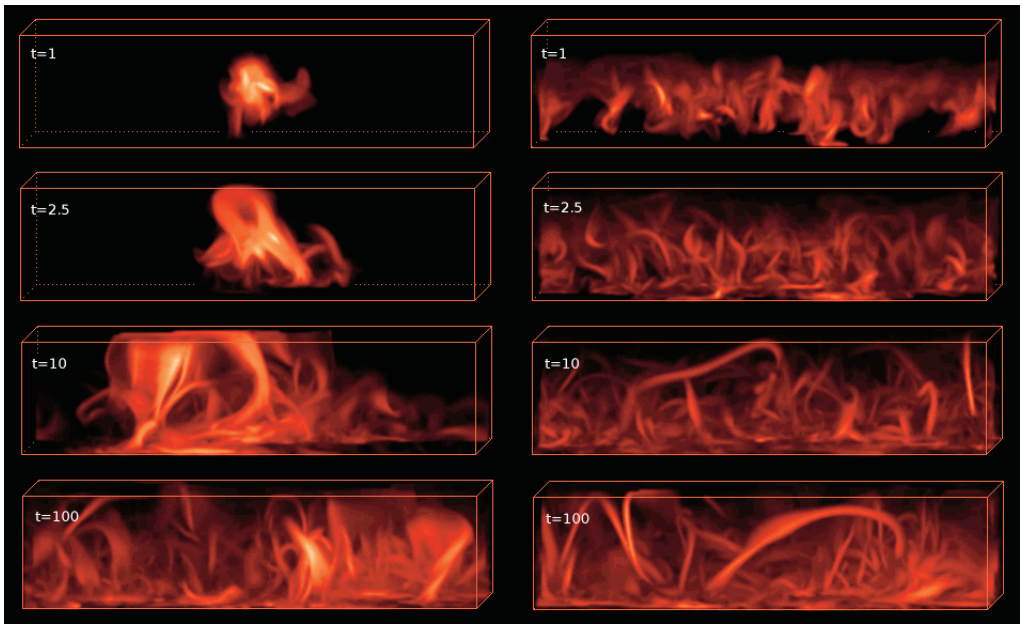

Figure 6. An MHD simulation from Abbett et al. (2004) showing the effects of turbulent convection on a relatively weak active region magnetic fields. Shown on the left is a volume rendering of $|\mathbf{B}|$ at four times during a simulation initialized with an untwisted flux tube aligned in the $\hat{\mathbf{x}}$ direction (z increases vertically, y increases from right to left, and x increases into the page). Shown on the right is a similar rendering for a simulation that began with a thin, horizontal layer of magnetic flux.

absence of the overshoot layer at the base of the simulation domain, this pumping mechanism is relatively weak. Of course in the presence of an overshoot layer, magnetic field entrained within strong downdrafts will penetrate into the stable layers and will be prevented from being re-circulated in the broad, slower moving upflows. Thus, magnetic flux can quickly accumulate in the overshoot layer and the amount of flux stored in the convectively unstable layers will be rapidly reduced.

5. Simulations of Active Regions at and Above the Photosphere

In order to connect simulation results directly to observations of the magnetic field at the photosphere, fully compressible, three-dimensional MHD simulations are required. There are two approaches that can be taken to modeling the surface layers: one can attempt to treat the energetics as realistically as possible, and generate results that can be directly compared to high resolution observations (*e.g.*, Bercik et al. 2003; Carlsson et al. 2004), or one can employ a more idealized approach (*e.g.*, Magara & Longcope 2001; Fan 2001; Abbett & Fisher 2003; Magara 2004; Manchester et al. 2004; Fan & Gibson 2004). The former can be computationally expensive, which puts practical limits on the size of the

computational domain. The latter approach relaxes this restriction, but the data so generated do not admit to a direct, detailed comparison with observations.

Simulations of active region magnetic fields that include the sub-photospheric layers of a turbulent convection zone and extend out into the solar corona are particularly challenging, and present a number of technical obstacles that must be overcome. First, there are inherent spatial disparities in the system — one must resolve a 100 km photospheric pressure scale height (the resolution requirements can be even more extreme, depending on how thermal conductivity in the transition region and corona is treated) in a domain that encompasses active region-scale magnetic features. Second, we are faced with significant temporal disparities: active regions in the photosphere evolve over time scales of weeks and months, while features in the magnetized corona can evolve over time scales of fractions of a second. Third, the physics of the coronal plasma fundamentally differs from the plasma of the lower atmosphere and interior: the corona is a field-filled, low-density, low-β (here, β refers to the ratio of the gas to magnetic pressure), magnetically-dominated plasma, while the convection zone is a turbulent, high-β plasma with strong, large-scale magnetic fields organized into isolated, magnetically-buoyant tube or rope-like structures, and small-scale fields concentrated in intergranular lanes and strong vortical downflows (see *e.g.*, Stein & Nordlund 2002; Stein et al. 2003; Fan et al. 2003; Abbett et al. 2004). In addition, the magnetized plasma of the chromosphere, transition region and corona can be shock-dominated (see *e.g.*, Carlsson & Stein 1992; Abbett & Hawley 1999; Roussev et al. 2004), while typical flow speeds in the lower layers of the convection zone tend to remain well below the characteristic sound or Alfvén speed (allowing for the anelastic treatment of active region fields in the interior; see Fan et al. 1999; Abbett et al. 2000, 2004). Finally, the computational domain must span over a 20 order of magnitude change in gas density, and a thermodynamic transition between the 1MK optically thin coronal plasma, and the optically thick cooler layers of the lower atmosphere and interior.

Work is underway to address each of these challenges, with the goal of being able to couple models of the deep interior to a self-consistent large-scale numerical model of the layers extending from two to four Mm below the visible surface out into the solar corona. We are now testing a code capable of solving the resistive MHD system of equations in these layers with a more sophisticated treatment of the energy equation than is typical of active region-scale models to date (see Figure 7). Spatial disparities are resolved using the adaptive mesh refinement (AMR) and domain decomposition library PARAMESH (MacNeice et al. 2000). Temporal disparities are addressed using a semi-implicit temporal discretization. The ideal portion of the system is evolved via the semi-discrete formalism of Kurganov & Levy (2000) with numerical fluxes calculated using the high-order, central weighted essentially non-oscillatory scheme of Levy et al. (2000) (this provides us with an excellent shock capture scheme, freeing up the AMR capability of PARAMESH to focus in on other physically interesting magnetic features in the solar atmosphere). The energy source terms (which in the corona include anisotropic thermal conduction, optically thin radiative cooling, and a coronal heating function consistent with the empirical relationship of Pevtsov et al. 2003) are treated implicitly via a Jacobian-free Newton-Krylov solver (see *e.g.*, Knoll & Keyes 2003 and references therein for a description of this technique). Contributions to the energy equation due to optically thick

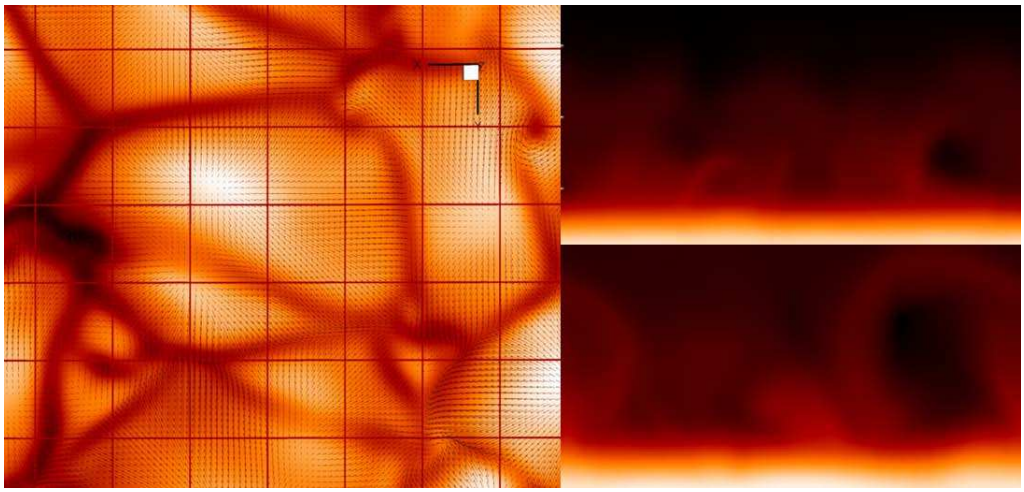

Figure 7. Early results from simulations whose domain encompasses both the upper layers of the solar convection zone and the magnetized corona. Left: A snapshot of the velocity during a relaxation run in a slice positioned just below the model photosphere. MPI block boundaries are shown. Right: $\log \rho$ (logarithm of the gas density) in the coronal portion of the computational domain along two different vertical slices (again, for a low resolution relaxation run).

radiative transitions are treated in an approximate, parameterized fashion, and radiation in the deepest layers of the computational domain is assumed consistent with the diffusion approximation with a temperature and density dependent Kramer's opacity.

6. The Past and the Future

Over the past decades, a substantial amount of progress has been made toward understanding the observational characteristics of active regions. As described above, both numerical simulations and theoretical models have been used to ascribe a physical basis for the equatorial zone of avoidance of active regions; active region orientations (Hale's Law and Joy's Law); the dependence of active region tilt on active region size; the dispersion of tilt versus active region size; asymmetric spot motions and morphological asymmetries; the helicity distribution of active regions with latitude, and the stability and cohesion of active region-scale magnetic flux ropes.

Yet much remains unknown — a new generation of more realistic large-scale numerical models are likely required to address such fundamental open questions as: Can we understand the transition between active region evolution that is described in terms of emerging flux tubes versus active region decay as described by passive flux transport models (Schrijver & Title 2001; Schrijver et al. 2002; Schüssler & Rempel 2005)? What is the triggering mechanism of CMEs and flares, and what role do photospheric flows, flux emergence and flux cancellation play in this process? If δ-spot active regions (non-Hale active regions that are often the source of the strongest eruptive events) are to be interpreted

as emerging flux ropes that have succumbed to the helical kink instability well below the surface (Linton et al. 1999; Fan et al. 1999), what is the source of such a large amount of twist? Can this twist be imparted by interactions of multiple flux systems (*e.g.*, Linton & Antiochos 2002)? How is the free energy from sub-surface fields transported into the corona? How do active region flux tubes interact with the small scale field in the Quiet Sun? With the rapidly increasing capabilities of computer hardware, and the increasing availability of computational resources, we look forward to further progress, and the answers to these and other open questions in the near future.

References

Abbett, W. P. & Fisher, G. H. 2003, ApJ, 582, 47
Abbett, W. P. & Hawley, S. L. 1999, ApJ, 521, 906
Abbett, W. P., Fisher, G. H., & Fan, Y. 2000, ApJ, 540, 548
Abbett, W. P., Fisher, G. H., & Fan, Y. 2001, ApJ, 546, 1194
Abbett, W. P., Fisher, G. H., Fan, Y., & Bercik, D. J. 2004, ApJ, 612, 557
Abbett, W. P., Mikić, Z., Linker, J. A., McTiernan, J. M., Magara, T., & Fisher, G. H. 2004, J. Atmos. Terr. Phys., 66, 1257
Antiochos, S. K., DeVore, C. R., & Klimchuk, J. A. 1999, ApJ, 510, 485
Bercik, D. J., Nordlund, A., & Stein, R. F. 2003, in ESA SP-517, SOHO12/GONG+ 2002. Local and Global Helioseismology: the Present and Future, ed. H. Sawaya-Lacoste, (Noorwijk: ESA), 201
Caligari, P., Moreno-Insertis, F. & Schussler, M. 1995, ApJ, 441, 886
Carlsson, M., Stein, R. F., Nordlund, Å., & Scharmer, G. B. 2004, ApJ, 610, L137
Carlsson, M. & Stein, R. F. 1992, ApJ, 397, L59
Cattaneo, F. & Hughes, D. W. 1988, J. Fl. Mech., 196, 323
Charbonneau, P. & MacGregor, K. B. 1997, ApJ, 486, 502
Choudhuri, A. R. 1989, Solar Phys., 123, 217
Corbard, T., Blanc-Féraud, L., Berthomieu, G., & Provost, J. 1999, A&A, 344, 696
D'Silva, S., & Howard, R. F. 1993, Solar Phys., 148, 1
D'Silva, S. & Choudhuri, A. R. 1993, A&A, 272, 621
Dikpati, M. & Charbonneau, P. 1999, ApJ, 518, 508
Dorch, S. B. F., Gudiksen, B. V., Abbett, W. P., & Nordlund, Å. 2001, A&A, 380, 734
Dorch, S. B. F. & Nordlund, Å, 2001, A&A, 365, 562
Emonet, T. & Moreno-Insertis, F., 1998, ApJ, 492, 804
Fan, Y. 2001a, ApJ, 554, L111
Fan, Y. 2001b, ApJ, 546, 509
Fan, Y. & Fisher, G. H. 1996, Solar Phys., 166, 17
Fan, Y. & Gibson, S. E. 2004, ApJ, 609, 1123
Fan, Y., Fisher, G. H., & Deluca, E. E. 1993, ApJ, 405, 390
Fan, Y., Zweibel, E. G., & Lantz, S. R. 1998, ApJ, 493, 480
Fan, Y., Zweibel, E. G., Linton, M. G., & Fisher, G. H. 1999, ApJ, 521, 460
Fan, Y., Abbett, W. P., & Fisher, G. H. 2003, ApJ, 582, 1206
Fisher, G. H., Fan, Y., & Howard, R. F., 1995, ApJ, 438, 463
Forbes, T. G. & Isenberg, P. A. 1991, ApJ, 373, 294
Forbes, K. F. & St. Cyr, O. C. 2004, Space Weather, 2, S10003
Getley, I. L. 2004, Space Weather, 2, S05002.
Hale, G. E., Ellerman, F., Nicholson, S. B., & Joy, A. H. 1919, ApJ, 49, 153
Knoll, D. A. & Keyes, D. E. 2003, J. Comp. Physics, 193, 357
Knowles, S. H., Picone, J. M., Thonnard, S. E., & Nicholas, A. C. 2001, Solar Phys., 204, 387
Kosovichev, A. G. 1996, ApJ, 469, L61

Kurganov, A. & Levy, D. 2000, SIAM J. Sci. Comput., 22, 1461
Lantz, S. R., & Fan, Y., 1999, ApJS, 121, 247
Levy, D., Puppo, G., & Russo, G. 2000, SIAM J. Sci. Comput., 22, 656
Linker, J. A., Mikic, Z., Titov, V., Lionello, R., & Riley, P. 2005, AGU Spring Meeting Abstracts, 5
Linton, M. G. & Antiochos, S. K. 2002, ApJ, 581, 703
Linton, M. G., Fisher, G. H., Dahlburg, R. B., & Fan, Y. 1999, ApJ, 522, 1190
Longcope, D. W. & Fisher, G. H., 1996, ApJ, 458, 380
Longcope, D. W., Fisher, G, H., & Arendt, S. 1996, ApJ, 464, 999
Longcope, D. W., Fisher, G. H., & Pevtsov, A. A. 1998, ApJ, 507, 417
Lynch, B. J., Antiochos, S. K., MacNeice, P. J., Zurbuchen, T. H., & Fisk, L. A. 2004, ApJ, 617, 589
MacNeice, P., Olson, K. M., Mobarry, C., de Fainchtein, R., & Packer, C., 2000, Comp. Phys. Comm., 216, 330.
Magara, T. & Longcope, D. W. 2001, ApJ, 559, L55
Magara, T. 2004, ApJ, 605, 480
Manchester, W., Gombosi, T., DeZeeuw, D., & Fan, Y. 2004, ApJ, 610, 588
Moreno-Insertis, F., Schüssler, M., & Caligari, P., 1994, Solar Phys., 153, 449
Moreno-Insertis, F. & Emonet, T. 1996, ApJ, 472, L53
Parker, E. N., 1979, Cosmical Magnetic Fields: Their Origin and Their Activity, (Oxford, England: Oxford Univ. Press)
Parker, E. N. 1993, ApJ, 408, 707
Pevtsov, A. A., Canfield, R. C., & Metcalf, T. R., 1995, ApJ, 440, L109
Pevtsov, A. A., Fisher, G. H., Acton, L. W., Longcope, D. W., Johns-Krull, C. M., Kankelborg, C. C., & Metcalf, T. R. 2003, ApJ, 598, 1387
Roussev, I. I., Sokolov, I. V., Forbes, T. G., Gombosi, T. I., Lee, M. A., & Sakai, J. I. 2004, ApJ, 605, L73
Schrijver, C. J. & Title, A. M. 2001, ApJ, 551, 1099
Schrijver, C. J., DeRosa, M. L., & Title, A. M. 2002, ApJ, 577, 1006
Schüssler, M. & Rempel, M. 2005, A&A, 441, 337
Spruit, H. C. 1981, A&A, 98, 155
Spruit, H. C. & van Ballegooijen, A. A. 1982, A&A, 106, 58
Stein, R. F. & Nordlund, Å. 2002, in ESA SP-505, SOLMAG 2002. Proceedings of the Magnetic Coupling of the Solar Atmosphere Euroconference, ed. H. Sawaya-Lacoste (Noordwijk: ESA), 83
Stein, R. F., Bercik, D., & Nordlund, Å. 2003, in ASP Conf. Ser. Vol. 286, Current Theoretical Models and Future High Resolution Solar Observations: Preparing for ATST, ed. A. A. Pevtsov & H. Uitenbroek, (San Francisco: ASP), 121
Tian, L., Liu, Y., & Wang, H. 2003, Solar Phys., 215, 281
Tobias, S. M., Brummell, N. H., Clune, T. L., & Toomre, J., 1998, ApJ, 502, L177
Tobias, S. M., Brummell, N. H., Clune, T. L., & Toomre, J., 2001, ApJ, 549, 1183
van Ballegooijen, A. A. 1982, A&A, 113, 99
van Driel-Gesztelyi, L. & Petrovay, K., 1990, Solar Phys., 126, 285
Wissink, J. G., Hughes, D. W., Matthews, P. C., & Proctor, M. R. E. 2000, MNRAS, 318, 501
Wright, J. M., Lennon, T. J., Corell, R. W., Ostenso, N. A., Huntress, W. T., Devine, J. F., & Crowley, P. 1995, "The National Space Weather Program: The Strategic Plan", Technical Report, Office of the Fed. Coord. for Meteorological Serv. and Supporting Res.